

# A 385-500 GHz 2SB SIS Mixer Based on a Waveguide Split-Block Coupler

Mamoru Kamikura<sup>1,2</sup>, Wenlei Shan<sup>2,3</sup>, Yu Tomimura<sup>1,2</sup>, Yutaro Sekimoto<sup>1,2</sup>, Shin'ichiro Asayama<sup>2</sup>, Naohisa Satou<sup>2</sup>, Yoshizo Iizuka<sup>2</sup>, Tetsuya Ito<sup>2</sup>, Toshiaki Kamba<sup>2</sup>, Yasutaka Serizawa<sup>1,2</sup>, and Takashi Noguchi<sup>2</sup>

**Abstract**—We have developed a 385-500 GHz sideband-separating (2SB) mixer, which is based on a waveguide split-block coupler at the edge of the E-plane of the waveguide, for the Atacama Large Millimeter/submillimeter Array (ALMA). An RF/LO coupler, which contains an RF quadrature hybrid, two LO couplers, and an in-phase power divider, was designed with the issue of mechanical tolerance taken into account. The single-sideband (SSB) noise temperature of a receiver using the RF/LO coupler is 104 K at the band center, which corresponds to 5 times the quantum noise limit ( $hfk$ ) in SSB, and 280 K at the band edges. The image rejection ratio of the receiver was found to be larger than 9.5 dB and typically 15 dB in the 385-500 GHz band.

**Index Terms**—sideband-separating (2SB) superconductor-insulator-superconductor (SIS) mixer, waveguide split-block coupler, RF quadrature hybrid, ALMA

## I. INTRODUCTION

The Atacama Large Millimeter/submillimeter Array (ALMA) [1] covers atmospheric windows from 30 GHz to 950 GHz in 10 frequency bands with relative bandwidth of 20-30 %. To improve the performance of the receiver, sideband separation is effective because it reduces the atmospheric noise [2].

Although there are several ways to achieve a 2SB mixer, we have selected a waveguide based 2SB mixer because it is compact, has no moving part, and good performance up to 370 GHz was reported by Claude (275-370 GHz) [3]. So far other waveguide based 2SB mixers were developed by Claude *et al.* (211-275 GHz) [4], Asayama *et al.* (90-115 GHz) [5], Chin *et al.* (86-116 GHz) [6], Vassilev *et al.* (85-115 GHz) [7], Kerr *et al.* (211-275 GHz) [8], Kamikura *et al.* (385-500 GHz) [9]. In this paper we present the recent results of the 2SB mixer for the 385-500 GHz band; compared to that described in [9], designs of an RF quadrature hybrid, an LO coupler, and the waveguide loads are revised.

A block diagram of a sideband-separating (2SB) mixer with two double-sideband (DSB) mixers is shown in Fig. 1, which is similar to that described in [3-9]. It consists of two DSB mixers, an IF quadrature hybrid, and an RF/LO coupler, which contains an RF quadrature hybrid, two LO couplers, an in-phase power divider, and three waveguide loads.

Manuscript received May 31, 2006.

This work was partially supported by Grant-in-Aid of JSPS No. 17340058.

<sup>1</sup>Department of Astronomy, School of Science, the University of Tokyo.

<sup>2</sup>Advanced Technology Center, National Astronomical Observatory of Japan, National Institutes of Natural Sciences, 2-21-1 Osawa, Mitaka-shi, 181-8588 Tokyo, Japan.

<sup>3</sup>Purple Mountain Observatory, Chinese Academy of Sciences, 2 West Beijing Road, Nanjing 210008, China.

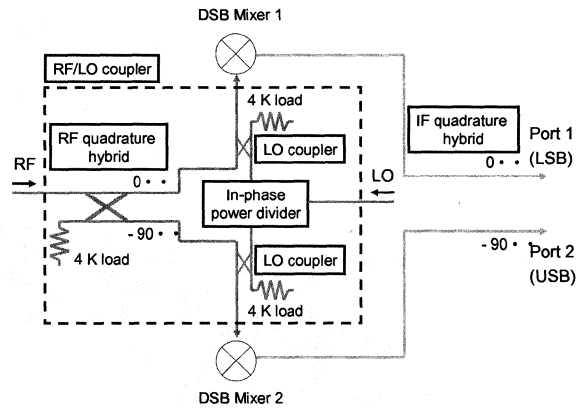


Fig. 1. Block diagram of a 2SB mixer [3-9]. RF/LO coupler contains an RF quadrature hybrid, two LO couplers, an in-phase power divider, and three waveguide loads.

## II. RF/LO COUPLER DESIGN

The design of an RF/LO coupler is shown in Fig. 2. To reduce the loss resulting from the misalignment of the two split blocks, the RF/LO coupler is split at the edge of the E-plane. At submillimeter wavelengths ( $\sim 0.6$  mm), the size of the waveguide and branch lines become smaller. The branch lines can be fabricated with electrical discharge machining. On the other hand, the waveguide itself can be made with direct machining. The alignment between the machining and electrical discharge machining is not easy. Since the alignment error degrades the performance of the 2SB mixer, split-block coupler at the edge of the E-plane was used. Compared with the split block in the middle of the E-plane as described in [3-8], the alignment of the two blocks becomes easier. We took care to ensure contact between the two blocks at the edge of the E-plane by arranging 4 screws effectively. The design is a scaled model described in [5] referring to [4]. The waveguide size of the RF/LO coupler is 559  $\mu$ m x 280  $\mu$ m (WR 2.2).

The unit of the RF/LO coupler were designed with a commercial 3D electromagnetic field simulator, HFSS (High Frequency Structure Simulator) [10]. We took into account conductor loss for the TE<sub>10</sub> mode because the higher modes are evanescent modes in the waveguide. The conductivity of gold at 4 K is assumed to be  $1.1 \times 10^9$  S/m, which includes the effect of the surface roughness ( $\sim 2$   $\mu$ m) of the waveguide as described in [11]. The conductor loss of the waveguide of the RF/LO coupler other than the RF quadrature hybrid and the LO coupler at 4 K was around 0.2 dB for the waveguide length of 20 mm.

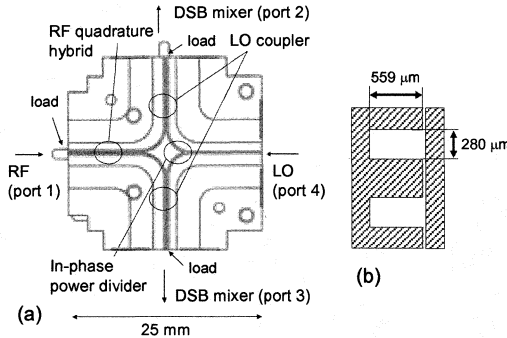


Fig. 2. (a) Design of the RF/LO coupler. (b) Close-up of the side view of the RF/LO coupler.

#### A. RF quadrature hybrid

An RF quadrature hybrid is a four-port coupler as shown in Fig. 3. The fourth port is terminated by a waveguide load. The two waveguides are separated by broad walls and are coupled through shunt guides approximately  $\lambda_g/4$  long. It is a 3 dB power divider with a 90 degree phase difference between the two outputs.

The RF quadrature hybrid was designed to have amplitude and phase imbalances of < 2.5 dB and < 10 degrees, respectively. These are required to achieve a 10 dB or larger image rejection ratio (IRR) of the 2SB mixer as described in [12].

The 58 μm width of the branch-line coupler was optimized from the electrical discharge machining. The number of branch lines and the dimensions were optimized as shown in Fig. 3. We have selected an 8 branch-line coupler.

At submillimeter wavelengths mechanical tolerance becomes very severe. The mechanical tolerance of the branch-line widths of the RF quadrature hybrid was studied in Fig. 4. We found that typical machining errors of ~ 5 μm do not affect the RF performance.

#### B. Waveguide load

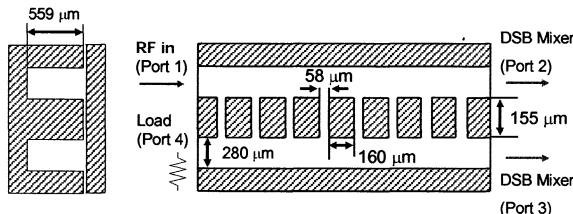


Fig. 3. Dimensions of the RF quadrature hybrid.

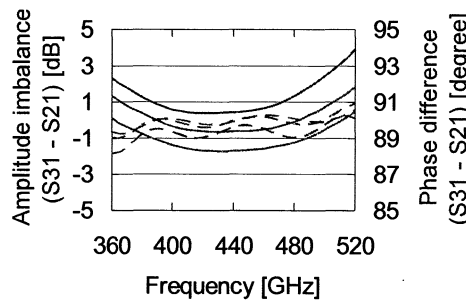


Fig. 4. Mechanical tolerance of the branch-line widths of the RF quadrature hybrid. The graph shows the amplitude imbalance and phase difference when no mechanical error exists (red lines) and the branch-line widths are smaller (blue lines) or larger (green lines) by 5 μm than the design values. Port definitions are as shown in Fig. 3.

For the material of the waveguide load of the RF/LO coupler, we have used MF116 [13], which is described in [14]. MF116 is made of iron powder and epoxy resin. The shape of the load is shown in Fig. 5 (a). Simulated input return loss of the load was as low as - 40 dB at 440 GHz as shown in Fig. 5 (b).

#### C. In-phase power divider

The in-phase power divider of the RF/LO coupler is an E-plane Y-junction. We have chosen to use an in-phase power divider of 3.0 mm radii. The input return loss of the in-phase power divider is < -24 dB from simulation.

#### D. LO coupler

From the point of view of an SIS mixer, lower coupling is desirable to minimize the loss of RF signals. However, the LO power is generally limited at the submillimeter wavelengths. In the case of this receiver, it was around 80 μW at the output of the cryogenic multiplier. Thus we have designed a -15 dB LO coupler with 3 slots as shown in Fig. 6. The mechanical tolerance of the slot widths of the LO coupler was studied as shown in Fig. 7. We found that typical machining error of ~ 5 μm do not affect the LO performance.

The 35 μm width of the slot was optimized from the electrical discharge machining. The number of slots and the dimensions of the LO coupler were optimized as shown in Fig. 6. The mechanical tolerance of the slot widths of the LO coupler was studied as shown in Fig. 7. We found that typical machining error of ~ 5 μm do not affect the LO performance.

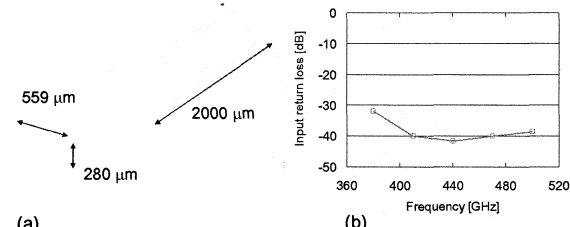


Fig. 5. (a) Shape of the waveguide load. (b) The simulated input return loss.

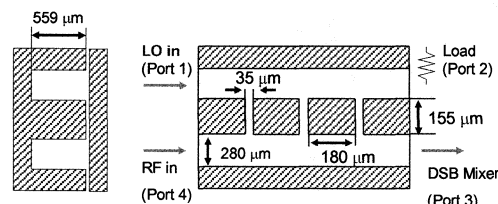


Fig. 6. Dimensions of the LO coupler.

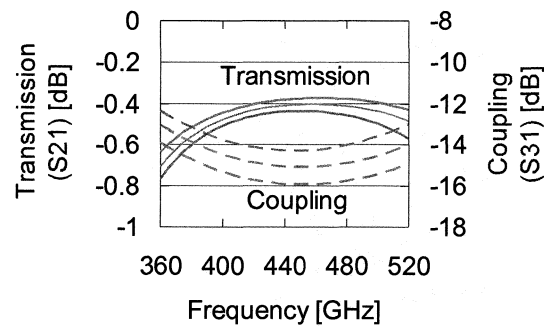


Fig. 7. Mechanical tolerance of the slot widths of the LO coupler. The graph shows transmission, and coupling when no mechanical error exists (solid lines) and the branch-line widths are smaller (blue lines) or larger (green lines) by 5 μm than the design values. Port definitions are as shown in Fig. 6.

### III. MEASUREMENT RESULTS

The RF/LO coupler was fabricated by Oshima Prototype Engineering [15]. The waveguide was made with direct machining and the branch lines were made with electrical discharge machining. The material is gold-plated TeCu. Three waveguide loads for the RF/LO coupler were made of MF116 [13].

Mechanical measurements with a microscope and measurements with a vector network analyzer (VNA) were done. The mechanically measured values were calibrated with a high precision scale, HL-250 [16]. The accuracy of the measurements was around 2  $\mu\text{m}$ , which was derived from the reproducibility of the measurements.

We have assembled a VNA for the 385-500 GHz band, using commercial components. Some S-parameters of the RF/LO coupler were measured with the VNA. The dynamic range is around 50 dB, and the amplitude and phase stability is around 0.1 dB and 1 degree in 1 hour, respectively.

To compare the measurements and the simulations at room temperature, we assumed that the conductivity of gold at room temperature is  $1.1 \times 10^7 \text{ S/m}$ , which includes the surface roughness ( $\sim 2 \mu\text{m}$ ) of the waveguide as described in [11].

#### A. RF quadrature hybrid

A 6 branch-line coupler, which is based on the design described in [9], was evaluated. From the mechanical measurement, a typical mechanical error was around 5  $\mu\text{m}$ . The measurements with the VNA at room temperature and simulation are compared as shown in Fig. 8. The maximum amplitude and phase imbalances were 1.7 dB and 12 degrees, respectively.

From simulation, the loss of the RF quadrature hybrid was -0.5 dB, the loss of the waveguide at room temperature was -1.4 dB, and the transmission of the LO coupler was -0.4 dB. For the simulation, we used the dimensions from the mechanical measurements. These results are consistent with the measured results with the VNA. The error bars were derived from the reproducibility of the measurements.

#### B. In-phase power divider and LO coupler

A 2 slot coupler, which is based on the design described in [9], was evaluated. We measured the insertion loss the LO coupler as shown in Fig. 9. The loss was found to be -20 dB at room temperature.

From simulation, the coupling of the LO coupler was -15.5 dB, the loss of the waveguide at room temperature was -1.4 dB, and the loss of the in-phase power divider was -3.1 dB. These results are consistent with the results from the measurements with the VNA.

## IV. RECEIVER PERFORMANCE

#### A. Cartridge-type receiver

A cartridge-type receiver [17] including the 2SB mixer was evaluated in a cartridge test cryostat [18]. The receiver consists of three cold stages with operating temperatures of 4 K, 15 K, and 110 K. A corrugated horn was designed by Matsunaga *et al.* [19]. CLNAs with 3-stage GaAs transistors and cryogenic isolators for the 4-8 GHz IF band have noise temperatures around 12 K. The coaxial cable was bent to connect between the DSB mixers and the IF quadrature hybrid, whose locations are not optimized.

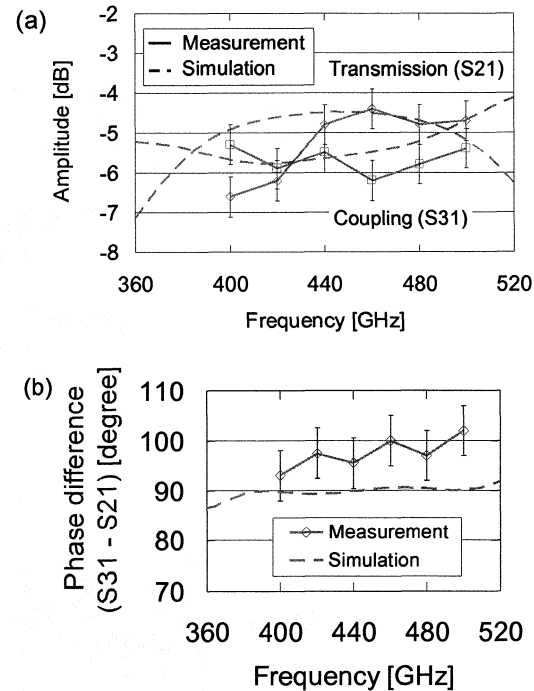


Fig. 8. Measured (solid line with points) and simulated (dashed line) results of (a) transmission and coupling of the RF quadrature hybrid, (b) phase difference of the RF quadrature hybrid. The error bars were derived from the reproducibility of the measurements. Port definitions are as shown in Fig. 2.

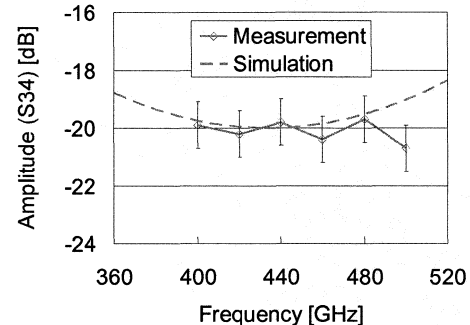


Fig. 9. Measured (solid line with points) and simulated (dashed line) results of the insertion loss of the LO coupler. The error bars were derived from the reproducibility of the measurements. Port definitions are as shown in Fig. 2.

The DSB mixer for the 385-500 GHz band has been developed by Shan *et al.* [20-21]. Two Nb-AlO<sub>x</sub>-Nb SIS (Superconductor-Insulator-Superconductor) tunneling junctions are parallel connected (PCTJ: parallel-connected twin junction [22]) as a tuning circuit in the DSB mixer.

The DSB mixer has a noise temperature as low as 3 times the quantum noise limit ( $h\nu/k$ ) with relative bandwidth of 20 %. Fig. 10 shows typical IV power curves of the DSB mixers. The superconducting magnet current was 10 mA to suppress the Josephson current of the SIS mixer. Josephson current is suppressed successfully.

The LO was a combination of a Gunn oscillator, a power amplifier, and a quintupler. The quintupler was mounted on the 15 K stage of the cartridge. On the other hand, the Gunn oscillator and the power amplifier were outside the vacuum vessel. The 78-100 GHz signal generated by the Gunn oscillator is amplified to  $\sim 100$  mW by the power amplifier.

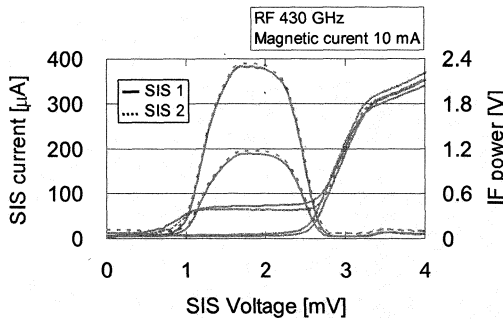


Fig. 10. Typical IV power curves of the DSB mixers

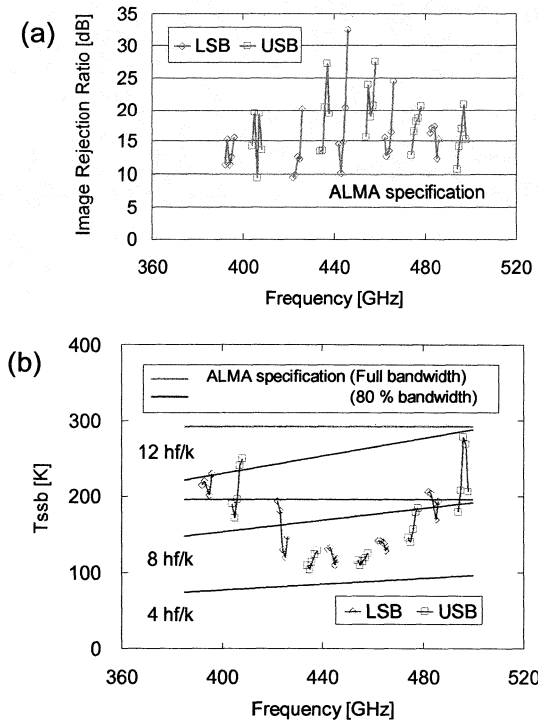


Fig. 11. (a) Image rejection ratio and (b) SSB noise temperature of the 2SB mixer measured with a cartridge-type receiver.

### B. Image rejection ratio and noise temperature

Image rejection ratio (IRR) was measured as shown in Fig. 11 (a) with the method from Kerr *et al.* [23]. The IRR was larger than 9.5 dB and typically 15 dB in the 385-500 GHz band.

The single-sideband (SSB) noise temperature of the cartridge for the 385-500 GHz band was measured with the Y-factor technique using a hot (300 K) and cold load (77 K) placed in front of the input window, as shown in Fig. 11 (b). The SSB noise temperature was 104 K around 435 GHz, which corresponds to 5  $hf/k$ , and less than 280 K in the 385-500 GHz band.

### ACKNOWLEDGMENT

We are grateful to Sheng-Cai Shi of Purple Mountain Observatory for collaborative developments of submillimeter receivers. The authors would also like to thank Junji Inatani, and members of ALMA-J.

### REFERENCES

- [1] R. L. Brown, W. Wild, C. Cunningham, "ALMA - the Atacama large millimeter array," *Advances in Space Research*, vol. 34, issue 3, pp. 555-559, 2004.
- [2] S. Guilloteau, "DSB versus SSB and Bandwidth/Sensitivity tradeoff," *ALMA Memo 393*, 2002.
- [3] S. Claude, "Sideband-Separating SIS Mixer for ALMA Band 7, 275-370 GHz," *Proc. 14th Int. Symp. on Space Terahertz Tech.*, 2003.
- [4] S. M. X. Claude and C. T. Cunningham, A. R. Kerr and S.-K. Pan, "Design of a Sideband-Separating Balanced SIS Mixer Based on Waveguide Hybrids," *ALMA Memo 316*, 2000.
- [5] S. Asayama, H. Ogawa, T. Noguchi, K. Suzuki, H. Andoh, and A. Mizuno, "An Integrated Sideband-Separating SIS mixer Based on Waveguide Split Block for 100 GHz Band," *ALMA Memo 453*, 2003.
- [6] C. C. Chin, D. Derdall, J. Sebesta, F. Jiang, P. Dindo, G. Rodrigues, *et al.*, "A Low Noise 100 GHz Sideband-Separating Receiver," *Int. J. Infrared and Millimeter Waves*, vol. 25, no. 4, pp. 569-600, 2004.
- [7] V. Vassilev, V. Belitsky, C. Risacher, I. Lapkin, A. Pavolotsky and E. Sundin, "A Sideband Separating Mixer for 85-115 GHz," *IEEE Microwave and Wireless Components Letters*, vol. 14, no. 6, pp. 256-258, 2004.
- [8] A. R. Kerr, S.-K. Pan, E. F. Lauria, A. W. Lichtenberger, J. Zhang, M. W. Pospiezsalski, *et al.*, "The ALMA Band 6 (211-275 GHz) Sideband-Separating SIS Mixer-Preamplifier," *Proc. 15th Int. Symp. on Space Terahertz Tech.*, 2004.
- [9] M. Kamikura, Y. Tomimura, Y. Sekimoto, S. Asayama, W. L. Shan, N. Satou, *et al.*, "A 385-500 GHz sideband-separating (2SB) SIS mixer based on a waveguide split-block coupler," *Int. J. Infrared and Millimeter Waves*, in press.
- [10] Ansoft Corporation, <http://www.ansoft.com/>.
- [11] Ansoft HFSS, Maxwell Online Help System, pp. 298, 1996-2002 Ansoft corporation.
- [12] A. R. Kerr and S. -K. Pan, "Design of Planar Image Separating and Balanced Mixers," *Proc. 7th Int. Symp. on Space Terahertz Tech.*, pp. 207-219, Available as *ALMA Memo 151*, 1996.
- [13] Emerson & Cuming Microwave Products, <http://www.eccosorb.co.jp/>.
- [14] A. R. Keer, H. Moseley, E. Wollack, W. Grammer, G. Reiland, R. Henry, *et al.*, "MF-112 and MF-116: compact waveguide loads and FTS measurements at room temperature and 5 K," *ALMA Memo 494*, 2004.
- [15] Oshima Prototype Engineering, <http://www.iijnet.or.jp/oshima/>.
- [16] Mitsutoyo Co., <http://www.mitutoyo.co.jp/eng/index.html>.
- [17] N. Satou *et al.*, "A submillimeter cartridge-type receiver for ALMA Band 8 (385 - 500 GHz)," in preparation.
- [18] Y. Sekimoto, T. Kamba, S. Yokogawa, M. Sugimoto, T. Okuda, R. Kandori, *et al.*, "Cartridge Test Cryostats for ALMA Front End," *ALMA Memo 455*, 2003.
- [19] M. Matsunaga, T. Matsunaga, Y. Sekimoto, "Analysis of submillimeter-wave horn antennas for submillimeter-wave telescopes," *SPIE*, vol. 5445, pp. 446-449, 2004.
- [20] W. L. Shan, T. Noguchi, S. C. Shi, Y. Sekimoto, "Design and Development of SIS Mixers for ALMA Band 8," *IEEE Trans. Appl. Superconductivity*, vol. 15, issue 2, pp. 503 - 506, 2005.
- [21] W. L. Shan, S. Asayama, M. Kamikura, T. Noguchi, S. C. Shi and Y. Sekimoto, "Development of a 385 - 500 GHz SIS mixer for ALMA band 8," *Proc. 16th Int. Symp. on Space Terahertz Tech.*, 2005.
- [22] S. C. Shi, T. Noguchi, and J. Inatani, "Development of a 500-GHz Band SIS Mixer," *IEEE Trans. Appl. Superconductivity*, vol. 7, issue 2, pp.2587-2590, 1997.
- [23] A. R. Kerr, S.-K. Pan and J. E. Effland, "Sideband Calibration of Millimeter-Wave Receivers," *ALMA Memo 357*, 2001.

